

Evidence of two competitive phenomena involved in the phase transition process at 144 K in K_2ZnCl_4 from x-ray diffraction and DSC experiments

This article has been downloaded from IOPscience. Please scroll down to see the full text article.

1995 J. Phys.: Condens. Matter 7 7651

(<http://iopscience.iop.org/0953-8984/7/39/007>)

View [the table of contents for this issue](#), or go to the [journal homepage](#) for more

Download details:

IP Address: 171.66.16.151

The article was downloaded on 12/05/2010 at 22:12

Please note that [terms and conditions apply](#).

Evidence of two competitive phenomena involved in the phase transition process at 144 K in K_2ZnCl_4 from x-ray diffraction and DSC experiments

A Hedoux, Y Guinet, F X Leduc, M More, M Foulon, F Danede and G Odou

Laboratoire de Dynamique et Structure des Matériaux Moléculaires, URA 801, UFR de Physique, Bâtiment P5, Université de Lille 1, 59655 Villeneuve d'Ascq Cédex, France

Received 9 June 1995, in final form 6 July 1995

Abstract. Differential scanning calorimetry and x-ray diffraction experiments performed in K_2ZnCl_4 have clearly revealed that two phenomena are involved in the phase transition process at 148 K. The first one corresponds to a slow reorganization of the tetrahedron configuration responsible for the development of a diffuse scattering localized on $(a^* + b^*)/2$ points of the reciprocal space. The second phenomenon corresponds to the growth of the $(a^* + b^*)/2$ superstructure phase. A very new feature results from observation of a competitive character between these two phenomena. It is shown that the kinetic behaviour of the first phenomenon and its possible correlation to the crystal growth defects are certainly involved in the phase transition process at 148 K.

1. Introduction

K_2ZnCl_4 is well known as an incommensurate insulator which undergoes the phase transition sequence normal–incommensurate–commensurate, commonly observed in the various A_2BX_4 -type ferroelectrics. However these materials exhibit some discrepancies in their low-temperature behaviour. If most of these compounds have a low-temperature phase below the commensurate phase, the phase transition process seems to be different. In Rb_2ZnCl_4 and K_2ZnCl_4 , the phase transition is associated with the softening of an optic mode, but Quilichini and coworkers have observed in these compounds two different behaviours of $\nu^2(T)$ for the soft optic branch [1]. In K_2ZnCl_4 this branch exhibits a minimum in $(\mu a^* + \frac{1}{2}b^*)$ which confirms the existence of an incommensurate phase found by Gesi. Several recent papers [2–5] report controversial hypotheses about this new incommensurate phase. This latter was found from dielectric [3], calorimetric [3] and neutron diffraction [2, 3] studies between 144.5 K and 148 K. More recent calorimetry experiments [4] and an x-ray study [5] performed on single crystals provided by Gesi have revealed the absence of an incommensurate phase just above the low-temperature phase.

On the other hand, different kinds of experiment (Raman spectroscopy [6, 7] on single crystals, DSC experiments [6, 7] and heat capacity measurement [8] on powder samples) have pointed out a slow transformation of the modulation below 250 K. Raman scattering experiments have shown a splitting of an extra-activated stretching mode at about 250 K. This mode is only predicted by superspace group theory and then it is closely connected to the modulation. As a consequence its splitting into two components reveals a change in the

characteristics of the modulation, i.e. a change in the configuration of the tetrahedra. This phenomenon is only observed via the study of internal stretching modes; no anomaly has been detected in the behaviour of lattice modes in the same temperature range. However a splitting of the low-frequency modes was observed only below 100 K [9], that has no correspondence with any reported phase transition. This observation has been interpreted as associated with a change in the lattice detected at 100 K instead of 144 K, because of the weak intensity of the distortion. Thermodynamic experiments [6–8] (DSC and calorimetry) performed on powder samples have also evidenced two different phenomena during a heating process of samples: a first-order phase transition at 144 K and a slow transformation between 147 K and 210 K. Our previous experimental investigations can be summarized as follows. In the low-temperature range (between 15 K and 300 K), two phenomena are observed: a very slow reorganization of the tetrahedra (between 148 K and ~ 250 K) corresponding to a change in the description of the modulation, and a phase transition at 144 K corresponding to a lattice distortion as was generally reported. In order to determine the possible correlation between the two phenomena and to clarify the ambiguity about the intermediate incommensurate phase observed between 144 K and 148 K, DSC and x-ray diffraction experiments were carried out on the same kind of single crystal.

2. Experimental details

Both kinds of experiment were carried out on single crystals grown from a slow evaporation of supersaturated aqueous solution of ZnCl_2 and KCl at room temperature.

Differential scanning calorimetry measurements were conducted on a Perkin–Elmer DSC 7 calorimeter. The calorimeter was calibrated for the different scanning rates studied, using the phase transition at 208.6 K in adamantane. A single-crystal mass of 41.85 mg was systematically analysed for different scanning rates ($0.5 \text{ K min}^{-1} \rightarrow 40 \text{ K min}^{-1}$) between 130 K and 290 K in cooling and heating runs.

X-ray diffraction experiments were performed on a four-circle diffractometer, using a Huber goniometer and a driving software developed in the laboratory. This device is very well adapted to the study of incommensurate phases and allows us to perform data collection through different methods: θ scans, θ – 2θ scans and Q scans for Bragg and satellite lines. The last of these methods was used to study $(a^* + b^*)/2$ superstructure lines. The study was performed between 110 K and room temperature using an N_2 gas flow low-temperature system which keeps temperature fluctuation within ± 0.5 K. The low-temperature device imposes $\theta_{\text{max}} = 14^\circ$ and the diffractometer equipment with Mo $K\alpha$ radiation corresponds to the limit value of $\sin \theta / \lambda < 0.34 \text{ \AA}^{-1}$. Experiments were performed on two samples: a platelet specimen with dimensions about $3 \times 2 \times 2 \text{ mm}^3$ and a spherical sample ($\varnothing \simeq 0.5 \text{ mm}$).

3. Results

3.1. Differential scanning calorimetry

Experiments performed in heating runs (figure 1) reveal clearly two different phenomena, as expected from previous calorimetry results [6–8] obtained on powder samples.

(i) A sharp peak is observed at the same temperature $T = 142 \text{ K} \pm 1 \text{ K}$ for all the scanning rates. Consequently this phenomenon does not exhibit a temporal dependence in spite of the differential enthalpy decreasing with decreasing scanning rate (table 1). This peak is associated with the first-order phase transition between the $c^*/3$ and $(a^* + b^*)/2$

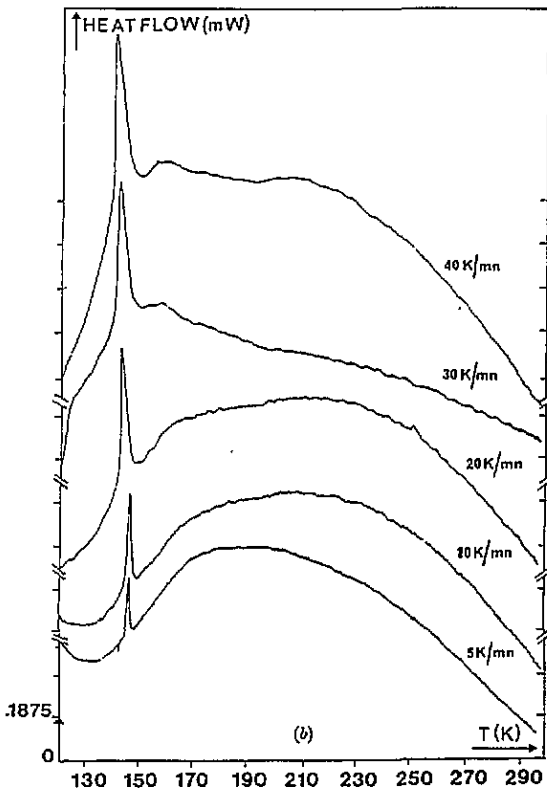
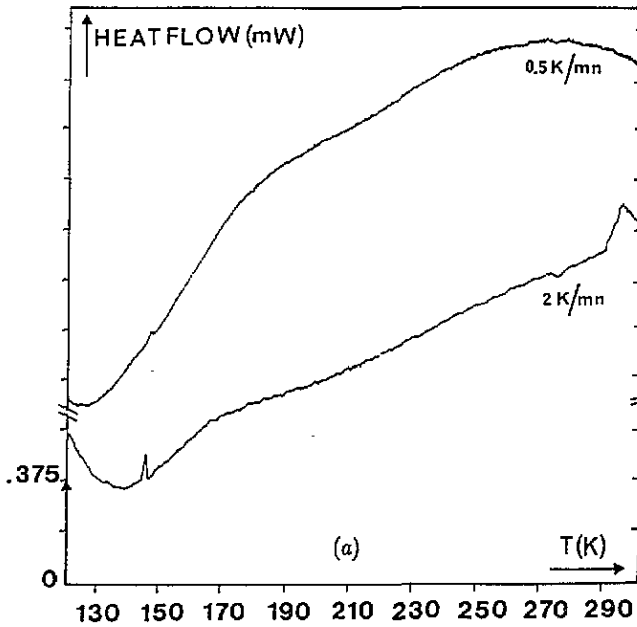


Figure 1. The evolution of heating run thermograms versus the scanning rate. All thermograms are plotted in the same heat flow range, taking into account the temperature shift due to the change of scanning rate. (a) Between 0.5 K min^{-1} and 2 K min^{-1} ; (b) between 5 K min^{-1} and 40 K min^{-1} .

Table 1. Values of differential enthalpy determined from cooling and heating run processes and versus the scanning rate.

Scanning rate (K min ⁻¹)	ΔH (J mol ⁻¹), heating run	ΔH (J mol ⁻¹), cooling run
0.5	+11 ± 1	indeterminate
2	+18 ± 1	-14 ± 1
1	+15 ± 1	-12 ± 1
5	+26 ± 1	-23 ± 1
10	+28 ± 1	-25 ± 1
20	+30 ± 2	-27 ± 2
30	+30 ± 2	-30 ± 2
40	+30 ± 2	-30 ± 2

superstructures.

(ii) A second phenomenon spreads out over the whole scanning temperature range (130–290 K) and exhibits a strong temporal shift versus scanning rate. It corresponds to a slow phase transformation which has been observed in powder experiments and interpreted as slow reorganization of tetrahedra.

For the high values of scanning rate, the phenomena are separate and the transformation splits into several unfinished transformations, certainly because the scanning rate is faster than the rate of the tetrahedron rearrangement. Moreover the temporal shift of the slow transformation seems to be correlated with the variation of ΔH associated with the first-order phase transition. This observation shows that the two phenomena are correlated, and the complete realization of the phase transformation prevents the phase transition at 144 K.

Cooling runs (figure 2) point out the same correlation between the two phenomena, i.e. the transformation is responsible for the annihilation of the phase transition. The temperature of the first-order phase transition, corresponding to the sharp peak, is determined at 143 ± 1 K and shows no dependence on the scanning rate. As a consequence no thermal hysteresis is associated with this phase transition. Figure 2 shows that a slow temperature decrease favours the realization of the transformation at the expense of the very sharp peak associated with the phase transition at 144 K. The same figure (2(c)) highlights the fact that the crystal undergoes a first transformation as soon as the temperature is decreased below room temperature. This uncompleted transformation could be the origin of the successive transformations (also not completed) and then induce the phase transition at 144 K. This hypothesis is confirmed from consideration of the lowest scanning rate (-0.5 K min⁻¹). In this case, only one transformation is observed and the sharp peak is not observable.

From table 1 and figures 1 and 2, 20 K min⁻¹ appears as a critical value of the scanning rate. Below this value, in both heating and cooling processes, the phase transformation is observed on thermograms more markedly than for higher values, and as a correlation the ΔH values associated with the phase transition decrease with decreasing scanning rate. As a consequence it can be assumed that from a given state of the phase transformation, this one starts to annihilate the phase transition. This observation can be interpreted as a competition between two phenomena, one being favoured according to the scanning rate of cooling or heating processes. This competition results from the kinetic behaviour of the second phenomenon which generates the variation of the 144 K phase transition enthalpy (table 1). This enthalpy varies in direct ratio with the quantity of transformed matter in the corresponding phase transition process.

The comparison between experiments performed on powder and the reported ones

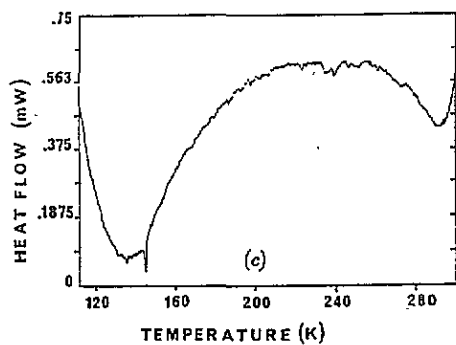
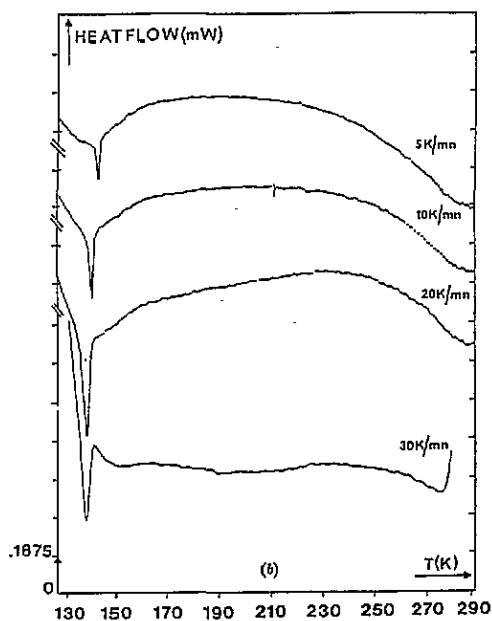
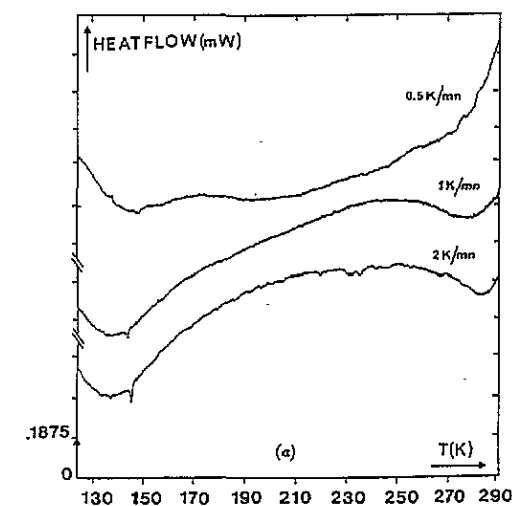


Figure 2. The evolution of cooling run thermograms versus the scanning rate. All thermograms are plotted in the same heat flow range, taking into account the temperature shift due to the change of scanning rate. (a) Between 0.5 K min^{-1} and 2 K min^{-1} ; (b) between 5 K min^{-1} and 30 K min^{-1} ; (c) T and heat flow rescaling of the thermogram recorded at 2 K min^{-1} .

carried out on single crystals reveals that the competition is only observed in single crystals. For any scanning rates in powder samples the two phenomena are simultaneously observed, the phase transition at 148 K being associated with the same constant value of $\Delta H = 30 \text{ J mol}^{-1}$. As a consequence the preponderance of the phase transformation is principally observed in single crystals. It can be assumed that the crystal growth defects could be at the origin of the competitive character between the two phenomena. To obtain an interpretation of each thermodynamic phenomenon, x-ray diffraction investigations were performed.

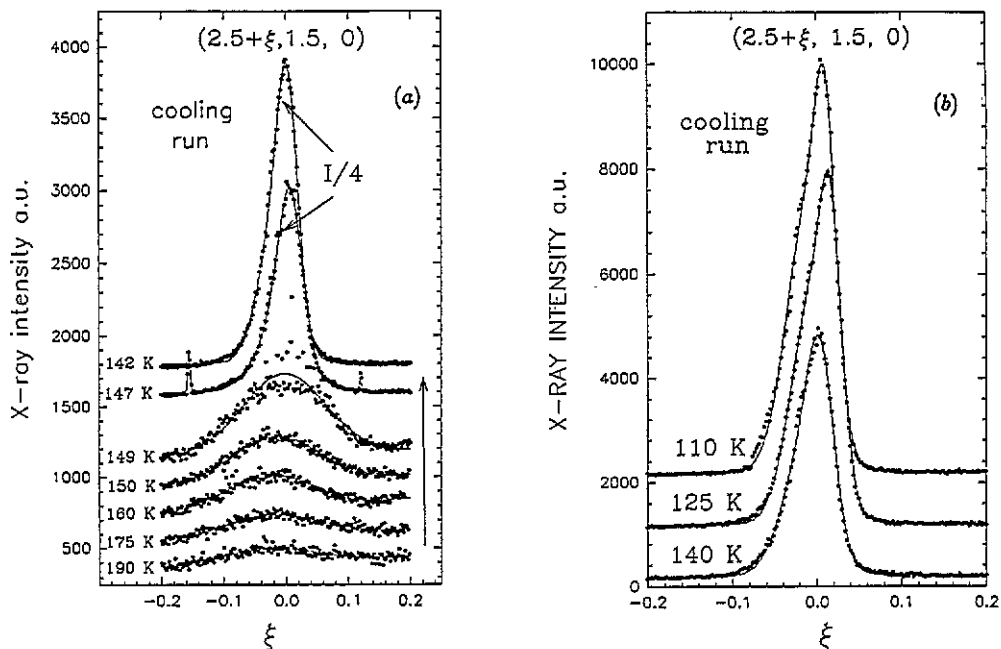


Figure 3. The temperature dependence of the x-ray diffraction profile for the $(2.5, 1.5, 0)$ scan along a^* (a) in the vicinity of the phase transition and (b) in the low-temperature phase.

3.2. X-ray diffraction experiments

The $(2.5, 1.5, 0)$ point of the reciprocal space was scanned along the a^* direction using the Q scan method between room temperature and 110 K (figure 3). These investigations were carried out first on a single crystal which had not undergone any thermal treatment. A very broad diffuse intensity was detected with temperature decreasing from 220 K, centred on the $(2.5, 1.5, 0)$ point. Its FWHM was determined from fitted data to be equal to 0.026 \AA^{-1} (3.7°) at 220 K. The temperature dependences of the intensity and the linewidth (FWHM) of the diffuse scattering are reported in figures 4 and 5 respectively. Figures 3–5 reveal a sudden sharpening of the diffuse scattering at 149 K with decreasing temperature which gives rise to a superstructure peak localized in an irrational position $(2.5 - \delta, 1.5, 0)$ with $\delta = 0.01$. At the same temperature a sharp peak emerges, also localized in an irrational position $(2.5 + \delta', 1.5, 0)$ with $\delta' \approx \delta$. Below 149 K, the x-ray intensity localized at $(2.5, 1.5, 0)$ is only correctly fitted using two Gaussian profiles. Thus, figure 3(b) confirms the coexistence of the two peaks down to 110 K through a marked asymmetric lineshape.

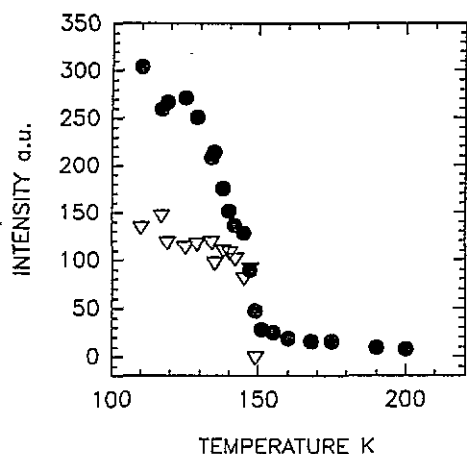


Figure 4. The temperature dependence of intensities of the diffuse scattering (full circles) and of the growing peak (open triangles).

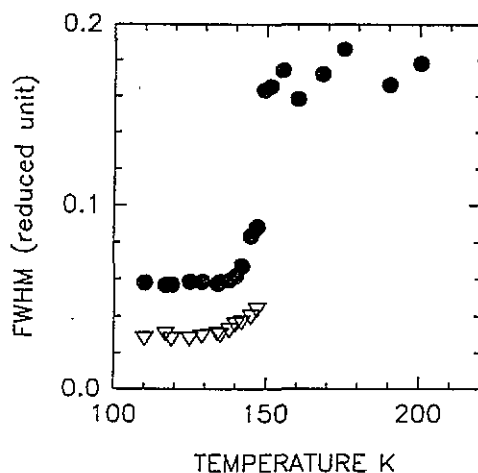


Figure 5. The temperature dependence of the FWHM for the diffuse scattering (full circles) and for the growing peak (open triangles).

Figure 4 shows a contrast between the temperature dependence of the intensity of the two lines below 149 K. The intensity I_1 of the peak which results from the sharpening of the diffuse scattering exhibits a strong temperature dependence compared to the behaviour of the growing peak I_2 . This figure reveals ($I_1 > I_2$) that the as-grown specimen is principally constituted below 144 K, by the phase resulting from the evolution of the diffuse scattering after a slow cooling at low temperature. The linewidth of the corresponding peak (figure 5) suggests that the low-temperature phase exhibits a very disorganized structure. However figure 4 shows that both linewidths exhibit no temperature dependence below 144 K, i.e. just below the phase transition. These results point out a critical temperature corresponding to the appearance of a superstructure line and to a sudden variation of the diffuse scattering characteristics (decreasing of linewidth and increasing of intensity). To determine what are the parameters at the origin of both lines, different thermal treatments were performed on the sample.

Table 2. Relative intensities of the diffuse scattering (I_1) and the growing superstructure peak (I_2) at 125 K after two different cooling run processes.

Cooling process	Diffuse scattering I_1 (%)	Superstructure peak I_2 (%)
Slow cooling	70	30
Quenching	38	62

By shifting the cold air stream, the sample was quenched from room temperature down to 125 K. The scan recorded after quenching is compared in figure 6 with the scan recorded after a slow cooling at the same temperature. This comparison evidenced an inverse ratio in the intensity of coexisting lines. The comparison between intensities (table 2) shows that the quench hinders the increase of the condensed diffuse scattering intensity (i.e. the growth of the δ quasicommensurate phase) whereas the growth of the δ' quasicommensurate phase is favoured.

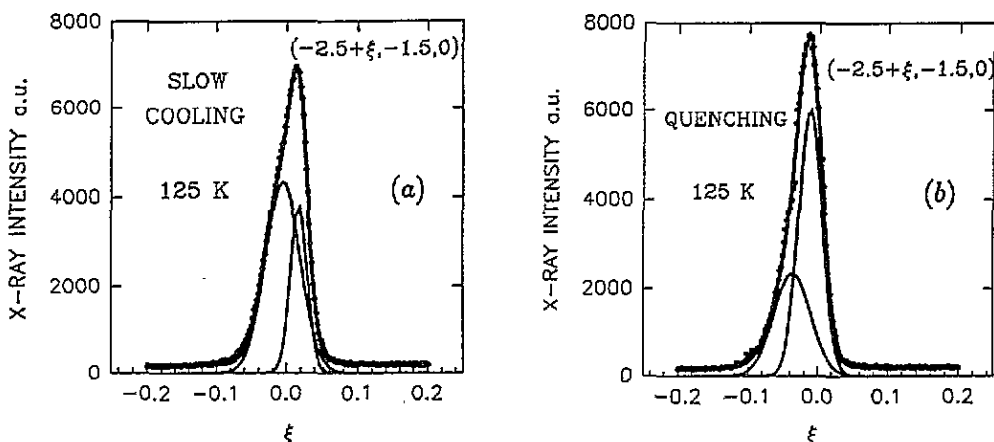


Figure 6. The x-ray diffraction profiles for the $(2.5, 1.5, 0)$ scan recorded (a) after a slow cooling and (b) after quenching.

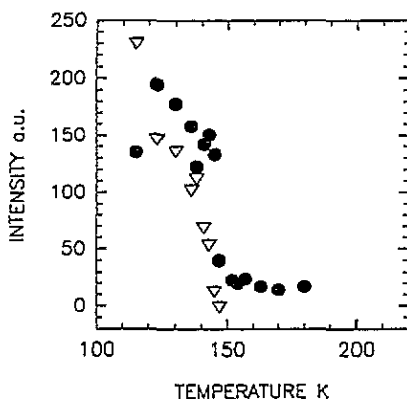


Figure 7. The temperature dependence of the diffuse scattering intensity (full circles) and the growing peak intensity (open triangles).

The sample was also annealed at about 363 K, and slowly recooled. The temperature dependence of the intensity of the coexisting lines is reported in figure 7. The comparison of figures 4 and 7 shows that the annealing process also favours the growth of the superstructure line at the low temperature. This phenomenon, clearly evidenced in figure 8, is certainly caused by the non-development of the diffuse scattering. It is clearly observed that the ratio I_1/I_2 is lower below the phase transition after annealing, and an inverse ratio is observed below 130 K. Consequently the quenching and annealing processes have the same influence on the low-temperature phase. In both cases the instantaneous phenomenon is favoured.

On the other hand, the different thermal treatments (quenching or annealing) which correspond to one of both dominant phenomena (the growing peak) involve localization of the growing superstructure towards a very closely commensurate position ($\delta' \rightarrow 0$), corresponding to the most stable configuration.

A second single crystal, which was characterized by a smaller size than the first, was investigated. For this sample, a diffuse scattering was also detected below 220 K on the same point in the reciprocal lattice. Figure 9 shows an increase of the intensity below 190 K down to 147 K. Figures 9 and 10 also reveal a coexistence of diffuse scattering and

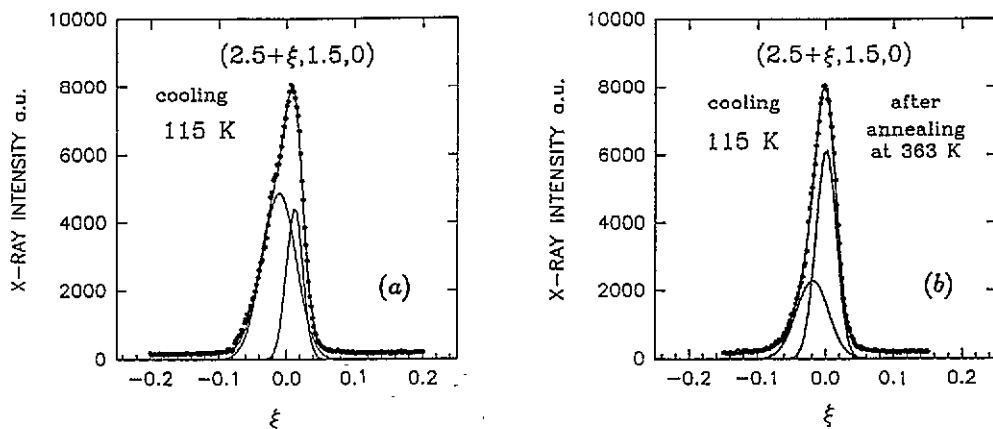


Figure 8. The x-ray diffraction profile for the $(2.5, 1.5, 0)$ scan recorded at 115 K on (a) the as-grown specimen and (b) the annealed specimen.

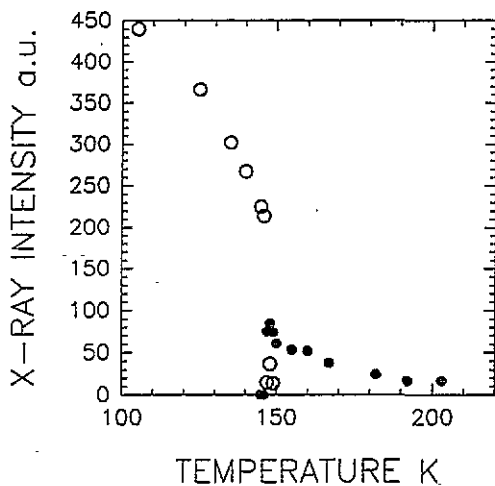


Figure 9. The temperature dependence of the diffuse scattering intensity (full circles) and the superstructure peak (open circles).

the growing superstructure line but only over few degrees. In this temperature range the diffuse scattering exhibits a critical behaviour. Its intensity undergoes a sudden decrease below 149 K after a marked increasing. This phenomenon is certainly correlated with the change of slope in the temperature dependence of the superstructure intensity.

In the two samples the appearance of the superstructure is observed at the same temperature (149 K). However in the second case the coexistence between the diffuse scattering and the growing sharp peak is observed only over a few degrees instead of a large temperature range as for the first sample.

The consideration of all experiments reported in this paper reveals that the non-development of the diffuse scattering involves the growth of a superstructure phase.

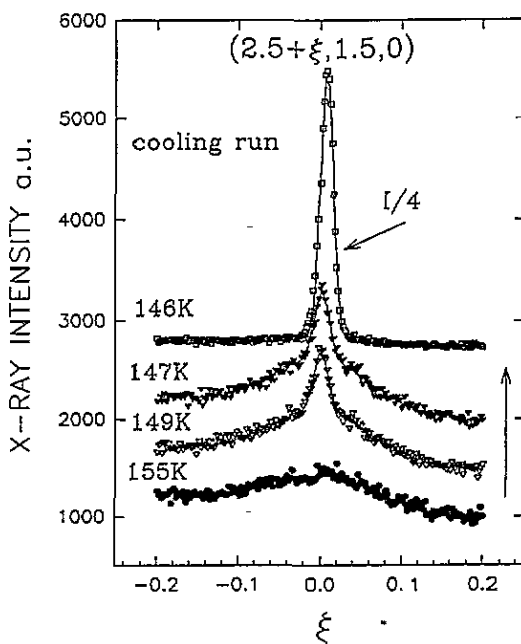


Figure 10. The x-ray diffraction profile of the $(2.5, 1.5, 0)$ scan versus temperature for the second smaller single crystal.

4. Discussion

The most attractive result of both DSC and x-ray diffraction experiments is the evidence of two competitive phenomena. From DSC experiments one of these phenomena is observed below about 250 K and spreads out down to about 100 K (for slow cooling, $v < 20 \text{ K min}^{-1}$). For high scanning rates, this phenomenon cannot spread out and thus exhibits a temporal behaviour. X-ray diffraction investigations reveal that this phenomenon corresponds to the growth of a broadened diffuse scattering localized on the positions corresponding to the $(a^* + b^*)/2$ superstructure lines of the low-temperature phase. These superstructure peaks are observed at 148 K and thus certainly responsible for the observation of the very sharp peak in the DSC experiments. However these superstructure peaks are not localized in a commensurate position, certainly because of the coexistence of a second peak resulting from diffuse scattering, and also localized in a quasicommensurate position. X-ray diffraction experiments confirm the kinetic behaviour of the spread phenomenon via the time dependence of its intensity which increases (at the expense of the growing sharp peak) on decreasing the cooling rate. DSC experiments show that 20 K min^{-1} could be a limit value for which one of the two phenomena is favoured at the expense of the other. It can be logically assumed that the spreading out of the diffuse scattering is favoured for slow cooling runs.

Another interesting phenomenon results from different observations in the low-temperature phase ($T < 148 \text{ K}$) in two different samples. In the first case a coexistence of two lines is observed, in accordance with DSC experiments. In the second case, a critical behaviour of the diffuse scattering is observed at 147 K. At this temperature, the growing superstructure line becomes more intense than the diffuse scattering which suddenly disappears. As a consequence only the superstructure line is observed in the low-temperature

phase. However, in both samples, 148 ± 1 K appears as a critical temperature because of behaviour of the sharpening of the diffuse scattering and the behaviour of the intensity of both diffuse scattering and superstructure line. Moreover, in both samples two phenomena are always observed, and below 148 K two different behaviours of the diffuse scattering are evidenced. These observations can explain the discrepancies reported in the literature concerning the phase transition at 148 K.

To understand the phenomenon associated with the peaks observed below 148 K, we have to consider the first modulation observed below $T_I = 553$ K and characterized by the wavevector $q\delta = (1 - \delta)c^*/3$. The structure determination of the INC phase in A_2BX_4 compounds [10, 11] has shown that the modulation can be interpreted by rotations of BX_4 tetrahedra around b and c directions (in the $Pm\bar{c}n$ setting). Previous Raman scattering studies on Rb_2ZnCl_4 [12, 13] and K_2ZnCl_4 [6] have pointed out new stretching modes below the N-INC transition, closely connected to the modulation and only predicted by four-dimensional group theory. In K_2ZnCl_4 , this mode splits into two components at about 250 K which has been interpreted as a rearrangement of the tetrahedron configuration. As a consequence, it can be assumed that the diffuse scattering corresponds to this rearrangement. The diffuse scattering and the growing peak at 148 K are localized in neighbouring positions, and thus reveal two similar rearrangements of tetrahedra. The detection of the very weak intensity in $(2.5, 1.5, 0)$ at about 220 K and the very broad diffuse scattering show the appearance of nuclei of a new modulated phase at this temperature. The growth of these nuclei exhibits different behaviours versus thermal treatment and also versus specimen of single crystals. This latter dependence shows that the crystal growth defects are certainly involved in the growing process of the nuclei. This interpretation can explain discrepancies reported for the phase transition around 145 K by different authors. However in every case a competitive character between two phenomena is observed in our experiments, in accordance with other recent x-ray diffraction experiments [5]. Electron microscopy study [14] has evidenced a high and inhomogeneous density of discommensurations at room temperature in samples prepared at room temperature. This observation reveals the presence of domains characterized by different $ZnCl_4$ orientations configured in a short-range order. The tetrahedra could be pinned to the crystal growth defects (modulation-defect interaction). Thus by decreasing the temperature, the defects can hinder the reorganization of tetrahedra towards a more stable configuration. The pinning of tetrahedra to the defects could be at the origin of the short-range order in the structural reorganization, i.e. at the origin of nuclei corresponding to the diffuse scattering. The competitive phenomena could result from hindrance to the growth of such nuclei at the expense of the growth of nuclei characterized by a closely similar tetrahedron configuration. Consequently the transition process into the low-temperature phase can be interpreted in terms of competition between the growth of two kinds of domain.

References

- [1] Quilichini M, Dvorak V and Boutrouille P 1991 *J. Physique I* **1** 1321
- [2] Gesi K 1990 *J. Phys. Soc. Japan* **59** 416
- [3] Gesi K 1992 *J. Phys. Soc. Japan* **61** 1225
- [4] Takai S, Atake T and Gesi K 1993 *J. Phys. Chem. Solids* **54** 213
- [5] Hasebe K, Asahi T, Kasano H, Mashiyama H and Kishimoto S 1994 *J. Phys. Soc. Japan* **63** 3340
- [6] Noiret I, Hedoux A, Guinet Y and Foulon M 1993 *Europhys. Lett.* **22** 265
- [7] Noiret I, Hedoux A, Guinet Y and Odou G 1994 *Ferroelectrics* **152** 343
- [8] Van Miltenburg J C, Noiret I and Hedoux A 1994 *Thermochim. Acta* **239** 33
- [9] Hedoux A, Noiret I, Guinet Y, Odou G and Lefebvre J 1992 *J. Chem. Phys.* **97** 6181

- [10] Hedoux A, Grebille D, Jaud J and Godefroy G 1989 *Acta Crystallogr. B* **45** 370
- [11] Quilichini M, Bernede P, Lefebvre J and Schweiss P 1990 *J. Phys.: Condens. Matter* **2** 4543
- [12] Katkanant V, Ullmann F G and Hardy J R 1985 *Japan. J. Appl. Phys.* **24** (Supplement 24-2) 790
- [13] Hedoux A, Guinet Y, Lefebvre J and More M 1991 *J. Chem. Phys.* **94** 7775
- [14] Pan X and Unruh H G 1990 *J. Phys.: Condens. Matter* **2** 323